

Effect of eigenmodes on the optical transmission through one-dimensional random media

H. Matsuoka and R. Grobe

Intense Laser Physics Theory Unit and Department of Physics, Illinois State University, Normal, Illinois 61790-4560, U.S.A.

(Received 17 May 2004; revised manuscript received 28 January 2005; published 8 April 2005)

Using the transfer matrix method as well as numerical solutions to the one-dimensional wave equation derived from the Maxwell equations, we study the transition from a photonic crystal with a finite size to a random dielectric medium. We examine the validity of the Kronig-Penney model for a finite size crystal and analyze the spatial structure of the eigenmodes as the crystal is made more irregular.

DOI: 10.1103/PhysRevE.71.046606

PACS number(s): 41.20.-q, 87.90.+y, 05.60.-k, 42.62.Be

I. INTRODUCTION

The propagation of electromagnetic radiation through highly scattering media can be described with three different degrees of accuracy. The least accurate approach uses the diffusion equation for which the optical properties of the medium are modeled by a single macroscopic parameter, the reduced scattering coefficient. More accurate is the description by the Boltzmann equation, in which the scattering phase function as well as the scattering coefficient model the medium. The Boltzmann and diffusion equations have been successfully applied in wide areas ranging from meteorology to bio-optical imaging. Both approaches approximate the radiation by its intensity and cannot describe any coherent phenomena that are based on the wave nature of the electromagnetic field. These two approaches give sufficiently accurate results for random media but are inappropriate for more regular structures such as are found in crystals.

The most accurate description of the radiation in regular structures is the microscopic approach provided by the Maxwell equations. It requires precise knowledge about the locations and optical properties of individual scatterers that constitute the medium. However, due to the complexity of this theoretical description, analytical solutions can be found only for systems that either consist of a very small number of scatterers or have simplifying geometries leading to reduced dimensional descriptions.

A lot of progress has been made on two separate fronts. The study of the band gap structures in photonic crystals [1] has led to remarkable potential applications for light switches and new optical filters. At the same time, the work on the quasicohherent properties of random media has resulted in the discoveries of light localization [2] and of lasing based on random media [3]. To the best of our knowledge, however, the precise nature of the transition from regular to random structures has not been thoroughly investigated.

In this work we will investigate this transition using the solutions of the Maxwell equations for a simple one-dimensional scattering system: a sequence of parallel dielectric slabs. The numerical solutions of these equations will permit us to explore the transition from a regular crystal, characterized by an equidistant arrangement of identical slabs, to a random system for which the index of refraction, the spacing between the slabs, or the thickness of the slabs is made random. We will examine the spatial structures of the corresponding eigenmodes and show that the change of the

total transmission coefficient is associated with a change in these modes. In a recent work [4], we have demonstrated that the transmission coefficient can be obtained directly from the eigenvalues of the stationary wave equation solved under an appropriate absorbing boundary condition. In this work our focus will be on the spatial properties of the eigenvectors.

This article is organized as follows. In Sec. II we describe our model system, the transfer matrix theory, and the numerical method with which we determine its spectrum and its eigenmodes. We also have a brief discussion on the physical meaning of these eigenmodes. In Sec. III we show how the transmission coefficient for a photonic crystal of a finite size is related to the spatial structure of the corresponding eigenmodes. We generalize the Kronig-Penney model, which has been used to model the electronic structure for a periodic potential, to the transport of electromagnetic radiation. We compare its prediction with our numerical results for the finite photonic crystal. In Sec. IV we introduce random fluctuations in various parameters of the dielectric medium and analyze their impact on the spectrum as well as on the eigenmodes. We close our discussion with an outlook on future work.

II. THE MODEL SYSTEM AND ITS NUMERICAL SOLUTION**A. The model system and the transfer matrix theory**

The model medium whose optical properties we will examine consists of a series of S lossless dielectric slabs arranged along the z axis. Each slab occupies an interval $[z_j - d_j/2, z_j + d_j/2]$ centered at z_j and has an index of refraction n_j ($j=1, 2, \dots, S$). The set of $3S$ numbers $\{z_j, d_j, n_j\}$ thus completely characterizes the medium. We neglect the homogeneous dispersion arising from a frequency-dependent index of refraction. However, due to the spatial dependence of the index of refraction from layer to layer, the net transmission strongly depends on the wavelength of the electromagnetic field.

We assume that the incoming field travels perpendicular to the slabs. This allows us to analyze the scattering of the field strictly in one dimension as the scattering is in either the forward or the backward direction and both the electric and magnetic field vectors are parallel to the slab-vacuum interfaces. In general, the electric field is a superposition of plane

waves polarized along the x direction, $\mathbf{E} = \mathbf{e}_x E \exp[i(\pm kz - \omega t)]$, where E is the complex amplitude and $k = 2\pi/\lambda$ denotes the wave number, while the magnetic field is a superposition of plane waves polarized along the y direction, $\mathbf{B} = \mathbf{e}_y B \exp[i(\pm kz - \omega t)]$.

For this model medium, we can compute the transmission coefficient exactly using the transfer matrix approach [5] by matching both the electric and the magnetic fields at the interfaces. For the j th slab occupying an interval $[z_j - d_j/2, z_j + d_j/2]$ and with an index of refraction n_j , the transfer matrix $\mathbf{M}^{(j)}$ relates the magnetic field $B(z) = B_a e^{ikz} + B_b e^{-ikz}$ on the left-hand side of the slab (i.e., for $z \leq z_j - d_j/2$) to the magnetic field $B(z) = B_c e^{ikz} + B_d e^{-ikz}$ on the right-hand side of the slab (i.e., for $z \geq z_j + d_j/2$) by

$$\begin{pmatrix} B_c \\ B_d \end{pmatrix} = \mathbf{M}^{(j)} \begin{pmatrix} B_a \\ B_b \end{pmatrix} = \begin{pmatrix} M_{11}^{(j)} & M_{12}^{(j)} \\ M_{21}^{(j)} & M_{22}^{(j)} \end{pmatrix} \begin{pmatrix} B_a \\ B_b \end{pmatrix}, \quad (2.1)$$

where

$$M_{11}^{(j)} = M_{22}^{(j)*} = e^{-id_j k} \left[\cos(n_j d_j k) + i \frac{n_j^2 + 1}{2n_j} \sin(n_j d_j k) \right] \quad (2.2a)$$

and

$$M_{12}^{(j)} = M_{21}^{(j)*} = -i \frac{n_j^2 - 1}{2n_j} e^{-2iz_j k} \sin(n_j d_j k). \quad (2.2b)$$

In between the slabs, the magnetic field amplitude does not change and the outgoing field amplitude B_c for the slab at z_j is identical to the incoming field amplitude B_a for the slab at z_{j+1} . For the medium composed of S slabs, we obtain the total transfer matrix by multiplying S transfer matrices, $\mathbf{M} = \mathbf{M}_S \mathbf{M}_{S-1} \cdots \mathbf{M}_3 \mathbf{M}_2 \mathbf{M}_1$. The total transmission coefficient T for the entire medium can then be computed from the total transfer matrix \mathbf{M} via $T = |\det \mathbf{M}|^2 / |M_{22}|^2 = 1 / |M_{22}|^2$, where M_{ij} are the matrix elements of \mathbf{M} .

B. Meaning of the eigenmodes

The eigenmodes for our medium are defined as those states $E_\omega(z)$ and $B_\omega(z)$ that satisfy the stationary wave equation for the electric field

$$-\frac{c^2}{n(z)^2} \frac{d^2}{dz^2} E_\omega(z) = \omega^2 E_\omega(z) \quad (2.3a)$$

and that for the magnetic field

$$-\frac{d}{dz} \left[\frac{c^2}{n(z)^2} \frac{d}{dz} \right] B_\omega(z) = \omega^2 B_\omega(z). \quad (2.3b)$$

In our work we are interested in the steady state inside the dielectric medium at a given laser frequency ω . In order to solve the eigenvalue problems, we must specify a set of boundary conditions for the second-order differential equations (2.3a) and (2.3b). For example, for the single periodic boundary condition [i.e., $E_\omega(-L/2) = E_\omega(L/2)$], the spectrum is in general nondegenerate. When we also require $dE_\omega/dz|_{z=-L/2} = dE_\omega/dz|_{z=L/2}$, it becomes discrete. For ab-

sorbing boundary conditions [i.e., $E_\omega(-L/2) = E_\omega(L/2) = 0$], the eigenvalues ω become also discrete. As we choose the numerical parameter L much larger than the size of the dielectric medium, the precise choice of the boundary condition is irrelevant for our discussion.

As the wave equation is of second order in time, the evolution of any initial electric field pulse $F(z, t=0) \equiv g(z)$ depends also on its initial time derivative $\partial F / \partial t|_{t=0} \equiv g_d(z)$. Using the eigenmodes, we obtain the time evolution of the electric field to be

$$F(z, t) = \sum_\omega \left[\langle E_\omega | g \rangle \cos(\omega t) + \frac{1}{\omega} \langle E_\omega | g_d \rangle \sin(\omega t) \right] E_\omega(z), \quad (2.4)$$

where the summation (or integration) extends over all positive frequencies and the notation $\langle | \rangle$ refers to the scalar product under which the eigenmodes are perpendicular to each other, $\langle E_\omega | E_{\omega'} \rangle = \delta_{\omega\omega'}$. We should note that in contrast to stationary energy eigenstates of the Schrödinger equation, whose norm is constant in time for a time-independent Hamiltonian operator, in the Maxwell case the weights are time dependent and there can be periodic moments in time when the factors $[]$ in front of $E_\omega(z)$ in Eq. (2.4) become identical to zero. As each term in the sum in Eq. (2.4) represents a standing wave, any propagating state must excite at least two different eigenmodes.

In a practical (time-dependent) arrangement, the incoming laser field would require some time for the steady state inside the dielectric medium to be established. During this time, the field energy density rises inside the dielectric medium as the laser light enters the medium. If this time is shorter than the time it takes for the front edge of the laser light to reach the numerical boundary at $z=L/2$ (or the reflected light to reach $z=-L/2$), then the time evolution given by the expansion in the eigenmodes describes the correct time evolution of the laser field. In other words, the (numerical) discreteness of the spectrum is irrelevant if L/c is chosen large enough.

C. Numerical technique to obtain the eigenmodes

We now discuss how we can determine the spatial profile of each eigenmode. We solve numerically the stationary wave equation for the magnetic field given by Eq. (2.3b) under absorbing boundary conditions. The magnetic field is polarized along the y axis, while the electric field is polarized along the x axis and related to the magnetic field through the Maxwell equations. We have discretized an interval $[-L/2, L/2]$ along the z axis into Q grid points located at $z_q = (-Q/2 - 1/2 + q)L/Q$, where $q = 1, 2, \dots, Q$. The discretized version of the wave equation (2.3b) takes the following form:

$$\begin{aligned} & \frac{1}{n(z_{q+1/2})^2} B(z_{q+1}) - \left[\frac{1}{n(z_{q+1/2})^2} + \frac{1}{n(z_{q-1/2})^2} \right] B(z_q) \\ & + \frac{1}{n(z_{q-1/2})^2} B(z_{q-1}) = k_j^2 \left(\frac{L}{Q} \right)^2 B(z_q). \end{aligned} \quad (2.5)$$

Using standard numerical techniques, we diagonalize the

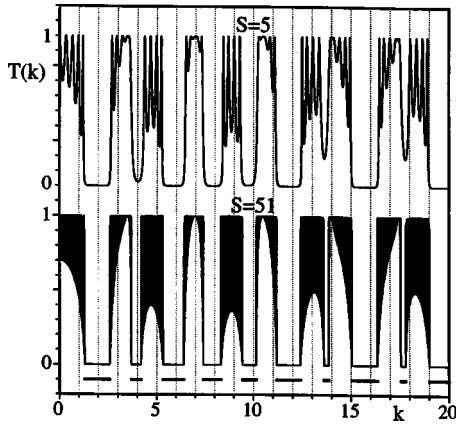


FIG. 1. The transmission coefficient for periodic arrays of 5 and 51 dielectric slabs as a function of the wave number k . The bars at the bottom indicate the locations of the band gaps according to the Kronig-Penney model. Each slab has an index of refraction $n_j=3$, a width $d_j=0.3$, and a position of $z_j=j-(S-1)/2$ ($j=1,2,3,\dots,S$).

tridiagonal matrix corresponding to this equation to compute its discrete eigenvalues k_j and eigenvectors.

For the special case of vacuum, for which $n(z)=1$, the eigenvalues of Eq. (2.5) can be obtained analytically as $k_j=(Q/L)[2-2\cos\{j\pi/(Q+1)\}]^{1/2}$. This expression is useful when we estimate the error due to the finite difference formula for the second derivative as well as due to the discrete sampling rate. Without discretization, the exact eigenvalues for vacuum for the interval of length L are given by $k_j=j\pi/L$ so that the density of eigenmodes defined as the average number of eigenvalues per unit wave number becomes $\rho(k)=L/\pi$.

III. THE SIMPLE PHOTONIC CRYSTAL WITH A FINITE SIZE

A. The transmission spectrum and the eigenmodes

Before we examine the transition from a regular photonic crystal to a random dielectric medium, let us first discuss the optical properties of a photonic crystal of finite size [6]. In Fig. 1, we display the transmission coefficient as a function of the wave number k for two photonic crystals consisting of $S=5$ and 51 dielectric slabs with a width of $d_j=0.3$ and an index of refraction $n_j=3$. We note that the alternating sequence of oscillatory intervals and regions with almost no transmission is characteristic for both systems and is rather independent of the system size S . The larger the system size S is, the more oscillatory is the transmission coefficient.

Let us take the case of $S=51$ to summarize the main features of the transmission spectrum. At $k=0$ (i.e., the static limit) the dielectric medium is invisible, or in other words, the wave with the corresponding (i.e., infinite) wavelength cannot resolve the presence of the medium. As the wave number grows, the transmission coefficient exhibits an oscillatory sequence of exactly S maxima at $T=1$, where S is the number of the slabs. With increasing k , the minima between the maxima descend until they reach $T=0$ at $k=1.31$.

In the next interval $1.315 < k < 2.594$, the medium is completely opaque, and this window of no transmission corre-

sponds to a band gap region for the photonic crystal of an infinite size, which will be discussed below. For $2.594 < k < 3.702$, we have again an oscillatory region, and for $3.702 < k < 4.182$ we have the next transmissionless region. This pattern repeats itself as k grows. We should point out that the overall structure of $T(k)$ does not depend too much on the crystal size S if S is larger than 5.

In order to relate the transmission coefficient to the discrete wave number spectrum, we have calculated the minimum spacing between adjacent eigenvalues defined as $s_j \equiv \min(|k_j - k_{j-1}|, |k_j - k_{j+1}|)$. As we mentioned above, for vacuum, the wave numbers are equidistant in the spectrum resulting in the constant density of eigenmodes $\rho(k)=L/\pi$. We find that the region with $T=0$ is characterized by pairs of degenerate wave number eigenvalues with $s_j=0$. In this region all the eigenmodes have practically vanishing weight inside the dielectric medium, $-S/2 < z < S/2$. Consequently, these eigenmodes have their support mostly on both sides outside the medium, which leads to the degeneracy. This finding is also consistent with the fact that for one-dimensional systems with reflection symmetry $n(z)=n(-z)$, the transmission coefficient is generally given by $T(k)=\sin^2[L\Delta(k)/2]$, where $\Delta(k)$ denotes the spacing between two adjacent eigenvalues [4]. It is also important to note that the density of eigenmodes is nearly constant for all k . The exceptions are the eigenmodes very close to the edges of the transmissionless regions where the density of eigenmodes becomes slightly higher. We will further comment on this in the next section. We also observe that the eigenmodes that are closest to these edges have a large weight inside the dielectric medium.

In Fig. 2, we display the spatial profiles of the eigenmodes near the first band edge at $k=1.315$ for the medium with $S=51$. For comparison we have also included the spatially dependent index of refraction at the bottom. Due to the reflection symmetry $n(z)=n(-z)$ for this regular array, the eigenmodes are either degenerate or with definite parity. The bottom and the top eigenmodes are degenerate, whereas the middle eigenmode has even parity. A comparison with Fig. 1 shows that the bottom eigenmode is associated with $T=1$, whereas the top two eigenmodes have vanishing transmission and nearly no weight inside the medium.

The bottom eigenmode with $k=1.313$ has a large fraction of its total weight inside the medium, whereas the eigenmodes for $k=1.327$ and 1.368 oscillate with an exponentially decaying amplitude inside the medium proportional to $B(z) \sim \exp[-(z+S/2)/D]$ in the region $-S/2 < z < 0$ and similarly for $z > 0$. Near a band edge, the decay length D is comparable in size to the length of the medium S , but as the wave number increases, the decay length shrinks. For a later comparison with the predictions by the Kronig-Penney model to be discussed in the next section, let us note that the numerically determined values for the decay length are $D \approx 4.7488$ for $k=1.327$ and $D \approx 2.3298$ for $k=1.368$.

B. The Kronig-Penney model for an infinite crystal

Let us now discuss a simple analytical model which can predict the locations of the transmissionless windows, where

$T(k)=0$, as well as the exponential decay lengths for the $T=0$ eigenmodes. We generalize the Kronig-Penney model [7] for an electron subject to a one-dimensional periodic step potential with the periodic boundary conditions to calculate the dispersion relation for an electromagnetic wave propagating through an array of equally spaced dielectric slabs of the fixed index of refraction. The stationary wave equation for the magnetic field polarized along the y axis was given by Eq. (2.3b), where the index of refraction n is periodic and satisfies $n(z+j)=n(z)$, where j is an integer. In each unit interval $[j, j+1]$, the index n takes the following two values: $n(z)=1$ ($j \leq z \leq j+1-d$) and $n(z)=n$ ($j+1-d < z \leq j+1$).

In the interval $0 < z < 1-d$, where $n(z)=1$, the magnetic field is given by $B=A_+e^{ikz}+A_-e^{-ikz}$, while in the interval $-d < z < 0$, where $n(z)=n$, the magnetic field is given by $B=C_+e^{inkz}+C_-e^{-inkz}$. We then look for an eigenmode with the ansatz $B(z \pm 1)=e^{\pm iq}B(z)$. If q is real, then it is called the crystal momentum of a Bloch wave. Matching the magnetic fields at $z=0$, we find $A_++A_-=C_++C_-$. Matching the electric fields or the derivatives of the magnetic fields at $z=0$, we also find $A_+-A_-=nC_+-nC_-$. Matching the magnetic fields at $z=1-d$, we find $A_+e^{ik(1-d)}+A_-e^{-ik(1-d)}=e^{iq}[C_+e^{-inkd}+C_-e^{inkd}]$, while matching the electric fields or the derivatives of the magnetic fields at $z=1-d$, we find $A_+e^{ik(1-d)}-A_-e^{-ik(1-d)}=ne^{iq}[C_+e^{-inkd}-C_-e^{inkd}]$. By putting these four equations for A_+ , A_- , C_+ , and C_- together, we obtain the following matrix equation:

$$\mathbf{A} \begin{pmatrix} A_+ \\ A_- \\ C_+ \\ C_- \end{pmatrix} = \begin{pmatrix} 1 & 1 & -1 & -1 \\ 1 & -1 & -n & n \\ e^{ik(1-d)} & e^{-ik(1-d)} & -e^{i(q-inkd)} & -e^{i(q+inkd)} \\ e^{ik(1-d)} & -e^{-ik(1-d)} & -ne^{i(q-inkd)} & ne^{i(q+inkd)} \end{pmatrix} \times \begin{pmatrix} A_+ \\ A_- \\ C_+ \\ C_- \end{pmatrix} = 0. \quad (3.1)$$

In order for a solution for this equation to exist, the determinant of \mathbf{A} , which is given by $\det \mathbf{A} = -4e^{iq}\{-(1+n^2)\sin(nkd)\sin[k(1-d)]+2n\cos(nkd)\cos[k(1-d)]-2n\cos q\}$, must vanish. If we define a new function $f(k)$ by

$$f(k) \equiv -\frac{n^2+1}{2n} \sin(nkd)\sin[k(1-d)] + \cos(nkd)\cos[k(1-d)], \quad (3.2)$$

the condition $\det \mathbf{A}=0$ becomes $f(k)=\cos q$. By solving this equation for a given value of q , we obtain the wave number k as a function of q [i.e., $k=k(q)$] as well as the dispersion relation or the frequency as a function of q [i.e., $\omega=ck=ck(q)$]. As $-1 \leq \cos q \leq 1$, those values of k for which $|f(k)| > 1$ do not lead to Bloch wave solutions. These k values form band gaps whereas those values of k for which $|f(k)| \leq 1$ form bands.

By solving either $f(k)=1$ or $f(k)=-1$, we can estimate the location of each band gap for a medium of infinite size with $d_j=0.3$ and $n_j=3$. The locations of the band gaps are indi-

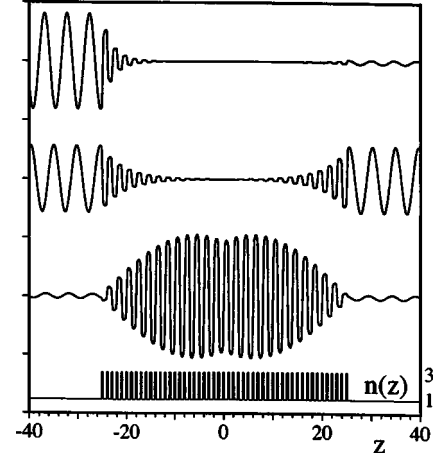


FIG. 2. Spatial profiles of the eigenmodes close to the border between a band and a band gap for a finite size crystal. The wave numbers for the eigenmodes are $k=1.313$ (bottom), 1.327 , and 1.368 (top). The bottom and top eigenmodes are degenerate; the middle one has even parity. The (numerically determined) exponential decay length for the $k=1.327$ and 1.368 eigenmodes are 4.7488 and 2.3298 , respectively. For comparison, we also show the spatially dependent index of refraction $n(z)$. [Each slab has an index of refraction of $n_j=3$, a width of $d_j=0.3$, and a position of $z_j=j-25$ ($j=1,2,3,\dots,51$). $S=51$, the numerical box length $L=200$, and $Q=20\,000$ leads to 30 grid points per slab.]

cated as solid bars below the curve for $T(k)$ for $S=51$ in Fig. 1 and the agreement with the numerical data for the two finite size systems is extremely good.

When $|f(k)| > 1$, q becomes either purely imaginary (i.e., $q=i \operatorname{Im} q$) or $q=\pi+i \operatorname{Im} q$ since $\cos(i \operatorname{Im} q)=\cosh(\operatorname{Im} q) > 1$ and $\cos(i \operatorname{Im} q + \pi)=-\cosh(\operatorname{Im} q) < -1$. The corresponding wave solution, for which $f(k) > 1$, then decays exponentially as $B_q(z)=e^{iqz}u_q(z)=e^{-(\operatorname{Im} q)z}u_q(z)$, where $\operatorname{Im} q=\cosh^{-1}[f(k)]$ and $u_q(z)$ is a periodic function that satisfies $u_q(z+1)=u_q(z)$. The wave solution, for which $f(k) < -1$, also decays exponentially as $B_q(z)=e^{iqz}u_q(z)=e^{-(\operatorname{Im} q)z}e^{i\pi z}u_q(z)$, where $\operatorname{Im} q=\cosh^{-1}[-f(k)]$.

We have estimated the decay lengths for the eigenmodes previously mentioned in Sec. III A. For the eigenmode at $k=1.327$, the Kronig-Penney model predicts $D_{\text{KP}}=1/\operatorname{Im} q=1/\cosh^{-1}[f(k)]=4.8526$, which roughly agrees with our numerical result $D \approx 4.7488$, whereas for the eigenmode at $k=1.368$, we find $D_{\text{KP}}=1/\operatorname{Im} q=1/\cosh^{-1}[f(k)]=2.3305$, which is in a better agreement with our numerical result $D \approx 2.3298$. As shown in Fig. 2, the eigenmode at $k=1.327$ decays into the medium more slowly with the longer decay length so that it suffers more severely from the finite size effect. This is why the agreement between D_{KP} and D is not as good for this eigenmode compared with the eigenmode at $k=1.368$.

The density of eigenmodes $\rho(k)$ also depends on the functional relationship between k and q as $\rho(k)=dN(k)/dk=(dk/dq)^{-1}[dN(k(q))/dq]$, where $N(k)$ is the number of the eigenmodes whose wave number is less than k . If we impose periodic boundary conditions on the index of refraction [i.e., $n(0)=n(S)$], then the eigenmodes must also satisfy the peri-

odic boundary conditions and the crystal momentum becomes an integer multiple of $2\pi/S$ or $q = (\text{integer}) \times (2\pi/S)$ so that $dN(k(q))/dq = S/\pi$ since for a given value of k , there exist two eigenmodes with $q = \pm(\text{integer}) \times (2\pi/S)$. The density of eigenmodes is then completely determined by the function $k=k(q)$ or $\rho(k) = (S/\pi)(dk/dq)^{-1}$. Because $(dk/dq)^{-1} = -(df/dk)/\sin q$, $(dk/dq)^{-1}$ diverges as k approaches a band edge, where $q = \pm\pi$, so that $\rho(k)/S$ diverges at the band edge as $\rho(k)/S \propto S$. In contrast, the density of eigenmodes that we have obtained for a finite dielectric medium of length S (embedded inside a larger interval of length L) is roughly independent of the wave number k except at the band edges, where it shows a small peak that grows with the medium size S . These peaks are therefore finite size effects and should lead to divergence as S grows to infinity.

As we will see in the next section, a different type of disorder introduced into a photonic crystal of finite size affects each band differently depending on how much amplitude weight the eigenmodes have in the dielectric slabs. Within the Kronig-Penney model, in order to estimate the relative overlap of an eigenmode with the dielectric slabs, we can use a ratio I_d/I_{1-d} between the average intensity of the magnetic field in a dielectric slab and the average intensity of the magnetic field in a gap between adjacent slabs defined as

$$\begin{aligned} \frac{I_d}{I_{1-d}} &= \frac{\int_{-d}^0 dz |B|^2}{\int_0^{1-d} dz |B|^2} \\ &= \frac{d(|C_+|^2 + |C_-|^2) + (1/nk)\text{Im}[C_+ C_-^* (1 - e^{-2inkd})]}{(1-d)(|A_+|^2 + 1) - (1/k)\text{Im}[A_+ (1 - e^{2ik(1-d)})]}, \end{aligned} \quad (3.3)$$

where $C_{\pm} = [-i/(n \mp 1)]\{e^{-i[q+k(1-d)]} - e^{\pm inkd}\}/\sin(nkd)$ and $A_+ = C_+ + C_- - 1$. For a medium of infinite size with $d_j=0.3$ and $n_j=3$, the ratios I_d/I_{1-d} for the first, the second, the fourth, the sixth, the eighth, and the ninth bands have a relatively larger value than for the third, the fifth, the seventh, and the tenth bands.

IV. IMPACT OF DISORDER ON THE EIGENMODES AND THE TRANSMISSION SPECTRUM

While there exist many studies on infinitely extended photonic crystals and completely random media, in this work we focus on the transition between these two limiting cases. There are various ways in which one can introduce disorder into the photonic crystal. Fluctuations can be introduced into each of the three parameters for the slabs: the index of refraction and the position and the width of each slab. It turns out that the resulting transmission spectrum depends sensitively on what kind of disorder is introduced. We will therefore discuss the specific impact of each kind of disorder separately and relate the transmission coefficient to the spatial structure of the eigenmodes.

The quasi periodic transmission spectrum for a perfect crystal was shown in Fig. 1. It was characterized by an al-

ternating sequence of regions with oscillating $T(k)$ (i.e., bands) and regions of zero transmission or gaps. The locations of these bands and gaps for media with a size $S > 5$ are predicted with remarkable precision by the Kronig-Penney model and are therefore found to be nearly independent of the system size. There are approximately two types of transmission bands in the spectrum. The third ($4.182 < k < 5.334$), the fifth ($8.328 < k < 9.446$), the seventh ($12.3966 \leq k \leq 13.6143$), and the tenth ($17.8016 \leq k \leq 19.0193$) bands are characterized by eigenmodes that have a relatively small overlap with each slab, which agrees with what the ratio I_d/I_{1-d} in the Kronig-Penney model indicates. We call these bands low bands. The eigenmodes of the first ($0 < k < 1.315$), the second ($2.594 < k < 3.702$), the fourth ($6.406 < k < 7.424$), the sixth ($10.150 < k < 11.198$), the eighth ($13.8595 \leq k \leq 15.055$), and the ninth ($16.3609 \leq k \leq 17.5564$) bands have a larger overlap with the slabs, which again agrees with what the ratio I_d/I_{1-d} in the Kronig-Penney model indicates, and we call these bands high bands. As a consequence of the different types of overlap between the eigenmodes and the slabs, the low and high bands are affected differently by disorder.

In general, fluctuations will reduce the transmission and the larger the wave number k is, the larger is the impact of fluctuations. In contrast to the periodic medium for which the overall transmission profile was nearly independent of the system size S , the effect of disorder is strongly dependent on the system size S .

However, as the size of fluctuations increases, we have also observed that within a region that is originally a very narrow band gap for the crystal, the value of the transmission coefficient can even evolve into a finite value. In fact, we have found a direct relationship between the size of the band and the required amount of disorder to induce a nonzero transmission. For example, a narrow gap ($3.702 < k < 4.182$) becomes transmissive for a lower degree of disorder than a relatively wider gap region ($5.334 < k < 6.406$). This is consistent with the spatial structure of the eigenmodes in a gap region whose exponential decay lengths D decrease as k approaches the center of the gap. Consequently the eigenmodes near the center of the gap have the smallest overlap with the medium and are most immune to disorder.

A. Disorder in the positions of the slabs

The location of each slab z_j was varied according to $z_j = j + r$, where r is a uniformly distributed random number in a range $-\zeta < r < \zeta$. The parameter ζ then serves as a measure for the degree of disorder in the positions. In order to avoid any overlap between two successive slabs, we have restricted ζ to be in the range $0 < \zeta < (1-d)/2$, where d is the width of each slab. In the third graph from the top in Fig. 3, we show the transmission coefficient $T(k)$ for $\zeta=0.34$ as a function of the wave number k . To better judge the impact of the fluctuations, we have also shown, at the bottom, $T(k)$ for the crystal taken from Fig. 1. A few observations are in order.

First, the first band is hardly affected by the position fluctuations, especially near $k=0$, simply because the eigenmodes near $k=0$ have wavelengths much longer than the

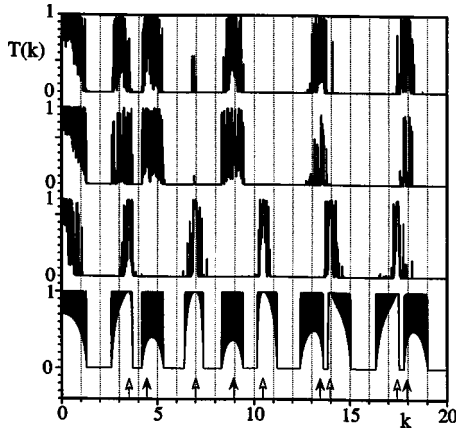


FIG. 3. The transmission coefficient for various types of disordered media for $S=51$. Index fluctuations (top): $n_j=3+0.3r$, $d_j=0.3$, $z_j=j-25$. Width fluctuations (second): $n_j=3$, $d_j=0.3+0.04r$, $z_j=j-25$. Position fluctuations (third): $n_j=3$, $d_j=0.3$, $z_j=j-25+0.34r$. Crystal (bottom): $n_j=3$, $d_j=0.3$, $z_j=j-25$. The random number r is uniformly distributed in $-1 < r < 1$. The open arrows denote locations $k_l=l\pi/(nd)$ and the closed arrows denote locations $k_l=l\pi/(1-d)$ for $l=1, 2, \dots$

distances between adjacent slabs and are therefore less sensitive to the actual positions of the slabs.

Second, the transmission coefficient for the third, fifth, seventh, and tenth bands (i.e., low bands) has been reduced to zero, whereas the second, fourth, sixth, eighth, and ninth bands (i.e., high bands) seem to be less affected by the position fluctuations. The reason for these remarkably robust eigenmodes in the high bands can be easily understood. The robust states are centered around those eigenmodes whose effective wavelength λ/n fits within twice the slab width d or $2d=l\lambda/n$, where l is an integer, so that $k_l=l\pi/(nd)$. For comparison, we have marked the locations of k_l by open arrows at the bottom of the figure. For these wave numbers, the field leaves each slab with a phase change of either 0 or π . In other words, these eigenmodes are completely immune to a change in the position of each slab because each slab becomes “invisible” for these eigenmodes and the corresponding transfer matrix for the slab [see Eq. (2.1)] becomes also diagonal. According to the Kronig-Penney model, the ratio I_d/I_{1-d} , which is the measure for the overlap of an eigenmode with the dielectric slabs, is $[d/(1-d)][(n^2+1)/(2n^2)]$ for the eigenmode with $k_l=l\pi/(nd)$, while $I_d/I_{1-d}=d/(1-d)$ for the eigenmode at $k=0$, which is the most resistant against disorder. For $n=3$, $(n^2+1)/(2n^2)=0.56$ is a sizable fraction of 1, which is consistent with our result that all the robust eigenmodes are found in high bands.

Using the Kronig-Penney model outlined in Sec. III B, one can show that in an infinite crystal the wave numbers $k_l=l\pi/(nd)$ are always located inside a band, because the function f in Eq. (3.2) takes the value $f(k_l)=(-1)^l \cos[k_l(1-d)]$ at this wave number so that the corresponding crystal momentum q_l satisfying $\cos q_l=f(k_l)=(-1)^l \cos[k_l(1-d)]$ is always real. We should remark that the appearance of these robust eigenmodes is a phenomenon unique to electromagnetic waves and there is no counterpart for electronic eigenstates for which the diagonal elements of the corresponding

transfer matrix vanish only at $k=0$. One could argue that these robust eigenmodes constitute a set of measure zero and are therefore irrelevant for $T(k)$ as a function of the continuous wave number k . However, due to the finite size of the medium, there are regions in k around k_l for which the transmission coefficient becomes sizable. The widths of these regions in k , however, shrink toward zero with an increasing system size.

B. Disorder in the width of each slab

Next we have varied the width of each slab d_j according to $d_j=d+r$, where r is again a uniformly distributed random number in a range $-\zeta < r < \zeta$. The second graph from the top in Fig. 3 shows the transmission coefficient for $\zeta=0.04$, for which each width was varied by at most $\zeta/d=0.13$. Different from the previous case, now the high bands are most sensitive to the fluctuations and for $\zeta > 0.04$ all but the first high band show a vanishing transmission. This is expected as the eigenmodes in the high bands have a larger overlap with the slabs and are therefore more sensitive to the changes in the slab widths.

C. Disorder in the index of refraction

Last we have varied the index of each slab n_j according to $n_j=n+r$, where r is a uniformly distributed random number in a range $-\zeta < r < \zeta$, where we set $0 < \zeta < 1-n$ to avoid a negative index of refraction. The top graph in Fig. 3 shows the transmission coefficient for $\zeta=0.4$ resulting in a relative fluctuation in the index of at most $\zeta/n=0.13$. The most robust eigenmodes are centered around the wave numbers $k_l=l\pi/(1-d)$ (l is an integer) marked in the figure by black arrows. This condition $k_l=l\pi/(1-d)$ means that an eigenmode associated with any of these wave numbers picks up only a phase of either zero or π in vacuum between a pair of adjacent slabs. As these special eigenmodes for our model medium are all found in the low bands and do not have much amplitude weight inside the slabs, the effect of disorder in the indices of refraction for the slabs are not much felt by these eigenmodes so that they are relatively robust against such disorder. These robust eigenmodes therefore see an effective homogeneous medium of length Sd , and if the index fluctuations are small, the transmission coefficient is that of a medium with length Sd and index n .

Returning to the Kronig-Penney model, we find that the function f in Eq. (3.2) reduces to $f(k_l)=(-1)^l \cos(ndk_l)$ so that the corresponding crystal momentum q_l satisfies $\cos q_l=f(k_l)=(-1)^l \cos(ndk_l)$. As $|\cos(k_l nd)| < 1$, we can always find a real value for q_l for each k_l so that these relatively robust eigenmodes are always inside a band.

V. SUMMARY AND OUTLOOK

We have investigated the effect of disorder on a one-dimensional photonic crystal with a finite size. Depending on the type of disorder introduced, different wave number regions in the transmission spectrum are affected by the disorder. We have traced the various impacts on the transmission spectrum back to the spatial structure of the eigenmodes,

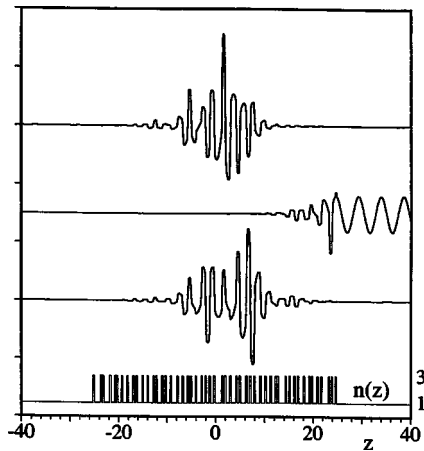


FIG. 4. Spatial profile of the eigenmodes for a random medium in the region with vanishing transmission. The wave numbers for the eigenmodes are $k=1.334$ (bottom), 1.355 (middle), and 1.376 (top). At the bottom is the spatially dependent index of refraction $n(z)$. [Each slab has an index of refraction of $n_j=3$, a width of $d_j=0.3$, and a random position of $z_j=j-25+0.34r$ where r is a random number in $-1 < r < 1$. $S=51$, the numerical box length $L=200$, and $Q=20\,000$ leads to 30 grid points per slab.]

which were obtained through a numerical solution of the stationary wave equation on a spatially discretized grid with the absorbing boundary condition. We have also generalized the Kronig-Penney model originally developed for an electron in a one-dimensional periodic potential to photonic crystals. This model provides an analytical insight into the basic features of the transmission spectrum, which persist even for finite size photonic crystals with a small amount of disorder. For a dielectric medium with reflection symmetry [i.e., $n(z)=n(-z)$], we have previously shown [4] that the transmission coefficient is directly related to the spacing between adjacent eigenvalues. In this work we have focused our attention on the effect of the spatial structure of the eigenmodes on the transmission spectrum.

Of some interest to us are the localized eigenmodes inside the medium that occur when the degree of disorder becomes significant. In a finite size random system, a vanishing transmission can be achieved either through degenerate states whose weights are basically outside the medium and which decay exponentially into the medium like evanescent waves or through nondegenerate normalizable localized states that reside inside the medium with no weight outside the medium. As an example, we show, in Fig. 4, the irregular spatial structure of two of these localized eigenmodes together with an exponentially decaying eigenmode (middle). We should also note that if the disorder is such that the parity in the index of refraction is still preserved [i.e., $n(z)=n(-z)$], then the localized states have either odd or even parity, or they are degenerate with partners that are their mirror images.

The present analysis was performed for a three-dimensional medium in which the special translation symmetry with respect to two coordinate directions led to an effectively one-dimensional description. This description permitted a straightforward application of the scattering matrices to obtain the transmission coefficient, the generaliza-

tion of the electronic Kronig-Penney model to the electromagnetic field situation and a relatively trivial diagonalization of the Maxwell steady state equation to compute the eigenvectors without extensive numerical calculation. Furthermore, the visualization of the results was significantly simplified leading also to a better intuition for the physics. The natural question that needs to be addressed concerns those finite sized random dielectric media that do not have any symmetries and require a full three dimensional treatment.

Even though some works have been reported on how to generalize transfer matrices to composite two- or three-dimensional (3D) systems [8–11], we are not aware how the Kronig-Penney model could be extended to describe these systems. Also the direct relationship [4] between the eigenvalue spacing of the discretized model and the transmission coefficient requires certain spatial symmetries for the 3D system in order to be valid.

However, despite the inapplicability of several mathematical and computational techniques, we believe that each of the physical findings in this work should also apply to systems that are truly random in all three spatial dimensions. For instance, the main connection between the degree of spatial localization of the eigenmodes and the corresponding transmission along that particular propagation direction as well as its sensitivity toward spatial randomness should obviously generalize to any nonsymmetric dielectric system as well.

In three-dimensional systems the eigenmodes are labeled by the vector \mathbf{k} (and not just the scalar k as discussed in this work) and only those modes can be excited by an incoming electromagnetic field, whose vector \mathbf{k} is approximately parallel to the propagation direction. Inside the medium, however, the beam can spread out (diffuse) significantly also in the two transverse directions. This transverse spreading behavior, however, cannot be predicted by our approach and would require the solution of the 3D Maxwell equation [12], as well as a corresponding diagonalization in all three spatial dimensions. We are not aware of any study that has investigated these interesting questions for a random medium of finite size.

As a first step one could investigate a two-dimensional photonic crystal of finite size, and explore how a randomness that acts only along one coordinate direction would affect the spatial structure of the eigenmodes in the perpendicular direction. It would be interesting to observe 3D localized states that require three different localization scales.

In a future work we will investigate the appearance of these localized eigenmodes as we increase the degree of disorder in a finite size crystal. As the corresponding eigenvalues will evolve through several avoided and possibly non-avoided crossings as the disorder grows, it might be interesting to trace localized states back to eigenmodes in the crystal. As the band gap eigenmodes for the crystal have practically no weight inside the medium, it might be interesting to observe how the localized eigenmodes are generated from these gap eigenmodes.

There are many more interesting questions for which one-dimensional model systems like the one studied in our analysis can be of help. For instance, it is not clear at the moment

how the randomness in the medium is reflected in the randomness of the corresponding (tridiagonal) matrix for the eigenmodes. Can one adopt some of the results of the theory of banded random matrices to better understand the transmission coefficient? Could one learn something from a level spacing statistics similar to those often investigated for quantum chaotic systems [13]? Is there a counterpart to the quantum chaotic systems characterized by a large amount of level repulsion? Maybe one can use the random matrix theory to identify the fluctuating part of the transmission coefficient to find its average, which then would be independent of the specific realization of the random medium. These questions are quite important when we try to make contact with more macroscopic theories for pulse propagation such as the Boltzmann theory mentioned in the Introduction. Even though a

strict mathematical derivation of the Boltzmann equation from the Maxwell equations has not been found [14], it was shown recently [15] that under certain conditions an average over a small frequency range of the Maxwell transmission data can match the prediction of the Boltzmann equation. A better understanding of the precise transition from a microscopic to a macroscopic theory would be very beneficial for the study of those systems that are too complex to be described by a microscopic theory but are too “coherent” to make the Boltzmann theory applicable.

ACKNOWLEDGMENTS

This work has been supported by the NSF. We also acknowledge support from the Research Corporation.

-
- [1] J. D. Joannopoulos, R. D. Meade, and J. N. Winn, *Photonic Crystals* (Princeton University Press, Princeton, N.J., 1995).
 - [2] A. Lagendijk and B. A. van Tiggelen, *Phys. Rep.* **270**, 143 (1996).
 - [3] S. John and G. Pang, *Phys. Rev. A* **54**, 3642 (1996).
 - [4] H. Matsuoka and R. Grobe, *Phys. Rev. Lett.* **91**, 130405 (2003).
 - [5] S. Menon, S. M. Mandel, Q. Su, and R. Grobe, *Opt. Commun.* **205**, 25 (2002).
 - [6] For our numerical study, the distance between the slabs becomes the unit for length, while setting $c=1$ fixes the unit for time so that the frequency ω and the wave number have the same value, $k=\omega$.
 - [7] See standard textbooks such as C. Kittel, *Introduction to Solid State Physics*, 7th ed. (John Wiley & Sons, New York, 1996).
 - [8] P. C. Waterman, *Phys. Rev. D* **3**, 825 (1971).
 - [9] B. Peterson and S. Ström, *Phys. Rev. D* **10**, 2670 (1974).
 - [10] S. Ström, *Phys. Rev. D* **10**, 2685 (1974).
 - [11] A. Quirantes and A. V. Delgado, *J. Quant. Spectrosc. Radiat. Transf.* **70**, 261 (2001).
 - [12] W. Harshawardhan, Q. Su, and R. Grobe, *Phys. Rev. E* **62**, 8705 (2000).
 - [13] F. Haake, *Quantum Signatures of Classical Chaos* (Springer-Verlag, Heidelberg, 1991).
 - [14] L. Mandel and E. Wolf, *Optical Coherence and Quantum Optics* (Cambridge University Press, Cambridge, U.K., 1995), Chap. 5.
 - [15] S. Menon, Q. Su, and R. Grobe, *Phys. Rev. E* **65**, 051917 (2002).